Improvement of Electronic Line-shafting Control in Multi-axis Systems

Chang-Fan Zhang[1]   Yuan-Yuan Xiao[1]   Jing He[1,2]   Min Yan[1]

[1]College of Electrical and Information Engineering, Hunan University of Technology, Zhuzhou 412007, China

[2]College of Mechatronic Engineering and Automation, National University of Defense Technology, Changsha 410073, China

Abstract: Electronic line-shafting (ELS) is the most popular control strategy for printing machines with shaftless drives. A sliding-mode controller for tracking control is designed in this study as the first step towards an improved ELS control scheme. This controller can eliminate the negative effects on synchronization precision resulting from the friction at low speed present in the pre-registration step of a shaftless driven printing machine. Moreover, it can eliminate the synchronization error of the printing process resulting from nonlinearities and load disturbances. Based on observer techniques, the unknown components of load torque and system parameter variations are estimated. On this basis, a novel ELS control method using equivalent load-torque observers is proposed. Experimental results demonstrate the effectiveness of the proposed control system for four-axis position control.

Keywords: Shaftless drive, sliding-mode controller, nonlinearity, observer, synchronization, position control, multi-axis system.

1 Introduction

High-precision synchronization control technology is extensively used in manufacturing industries such as printing, aerospace, textile, and steel rolling[1−3]. The higher precision design of it for system with nonlinearity and disturbances is the key to its application in manufacturing.

Traditional synchronization control strategies include master-slave control, cross-coupling control, relative-coupling control, and electronic line-shafting (ELS) control[4]. As a typical one among them, ELS is extensively used in engineering application due to its excellent synchronization performance[5, 6]. Lorenz[7] conducted extensive research in this area, and Payette[8, 9] also made contributions in ELS development. Valenzuela and Lorenz[10] described the physical meaning of ELS and applied it to printing machines. Based on the previous achievements, Perez[11] extended the study of ELS control strategy and perfected the ELS algorithm, Wolf and Lorenz[12] proposed compensation-based ELS control to eliminate the effect of tension on printing paper. Furthermore, improved tracking-control algorithms were developed to increase the synchronization precision of multi-axis systems[13, 14].

In a multi-axis motion system, synchronization is required in the case of load variation. Because the real load torque is time-varying and not measurable, existing ELS-based control strategies take the virtual load torque (i.e., the coupling torque) of each axis as their load torque feedback. These feedback signals act together on the virtual shaft to form a coordinated signal for the motion synchro-

nization of all the axes. Under steady-state conditions, this feedback control can provide excellent synchronization performance. However, if a severe unknown load disturbance occurs in the system, loss of synchronization among the axes probably happens. To address this problem, a novel ELS control strategy is proposed in this paper. By constructing an observer, the equivalent load torque is observed, and the observed value is directly fed back to the virtual shaft.

The paper is organized as follows: Section 2 describes a direct current (DC) motor system. Section 3 introduces the traditional ELS control method. Section 4 presents a novel ELS structure. Section 5 describes the control design. Section 6 presents experimental results and conclusions in Section 7.

2 Mathematical model of the system

Synchronous coordinated running of each printing roller of a shaftless-driven printing press is accomplished mainly by independent-drive servo motors. Register control is carried out if chromatic aberration occurs. This control scheme results in fast, accurate, and steady control of the system with respect to object position and velocity. There are many models of servo drive motors. But to reflect a practical implementation more precisely, it is desirable to take parameter variation, friction, and load torque into consideration in the model. Therefore, a DC motor is selected as the servo motor type. The dynamic system can be described by

$$
\begin{cases}
\dot{x}_1 = x_2 \\
\dot{x}_2 = -\dfrac{k_m c_e}{JR} x_2 + k_u \dfrac{k_m}{JR} u(t) - \dfrac{1}{J} F_f(t) - \dfrac{1}{J} \mathrm{T}_L
\end{cases}
\tag{1}
$$

where $x_1 = \theta$ is the angular position, $x_2 = \omega$ is the angular velocity, c_e is the voltage feedback coefficient, J is the inertia, R is the total armature resistance, k_m is the electromechanical torque coefficient, k_u is the pulse-width modulation (PWM) coefficient of amplification of the power amplifier, $u(t)$ is the control input, T_L is the load torque, and $F_f(t)$ is the friction. The mathematical model of $F_f(t)$ can be expressed as follows[15]:

When $\left|\dot{\theta}\right| < \sigma_1$, the static friction is

$$F_f(t) = \begin{cases} F_m & , \quad \text{if} \quad F_t > F_m \\ F_t & , \quad \text{if} \quad -F_m < F < F_m \\ -F_m & , \quad \text{if} \quad F_t < -F_m. \end{cases} \tag{2}$$

When $\left|\dot{\theta}\right| > \sigma_1$, the dynamic friction is

$$F_f(t) = [F_c + (F_m - F_c)\mathrm{e}^{-\sigma_2|\dot{\theta}|}]\mathrm{sgn}(\dot{\theta}) + k_v\dot{\theta}. \tag{3}$$

While the driving force $F(t)$ is

$$F(t) = J\ddot{\theta} \tag{4}$$

where F_m is the maximum static friction, F_c is the coulomb friction, k_v is the proportionality factor for viscous friction torque, and σ_1 and σ_2 are very small positive constants.

It is assumed that $\overline{a_1} = -\frac{k_m c_e}{JR}$, $\overline{b} = \frac{k_u k_m}{JR}$ and $\overline{a_2} = -\frac{1}{J}$ are three nomimal values. Considering parameter variation, (1) can be rewritten as

$$\begin{cases} \dot{x}_1 = x_2 \\ \dot{x}_2 = a_1 x_2 + bu(t) + a_2 F_f(t) + a_2 T_L \end{cases} \tag{5}$$

where $a_1 = \overline{a_1} + \Delta a_1$, $b = \overline{b} + \Delta b$, $a_2 = \overline{a_2} + \Delta a_2$, Δa_1, Δb and Δa_2 are uncertain items caused by the variation of parameters k_m, J and R.

Define $T_L^* = \Delta a_1 x_2 + \Delta bu(t) + \Delta a_2 F_f(t) + a_2 T_L$ as the equivalent load torque, then (5) can be rewritten as

$$\begin{cases} \dot{x}_1 = x_2 \\ \dot{x}_2 = \bar{a}_1 x_2 + \bar{b}u(t) + \bar{a}_2 F_f(t) + T_L^*. \end{cases} \tag{6}$$

3 Traditional ELS control

The mechanical shaft driven system provides power to each individual servo drive unit by means of a mechanical shaft and maintains their motion synchronization simultaneously. In the ELS control strategy, a virtual shaft is used to replace the mechanical shaft by realistically simulating its physical characteristics. Each axis follows the motion of the virtual shaft and couples with it by torque integration and feedback. When the signal from the virtual shaft control system is applied to the mechanical shaft, a reference signal for each unit controller is obtained. In other words, the reference input signal, instead of the system input signal, is synchronized among all unit controllers. Because it is a filtered signal applied to the shaft, it can be tracked more easily by the unit controllers, and can improve synchronization performance. The ELS control structure is shown in Fig. 1.

Fig. 1 shows that the virtual electric line shaft, known as the master, involves the adjustment of shaft velocity or position and provides the velocity or position reference value
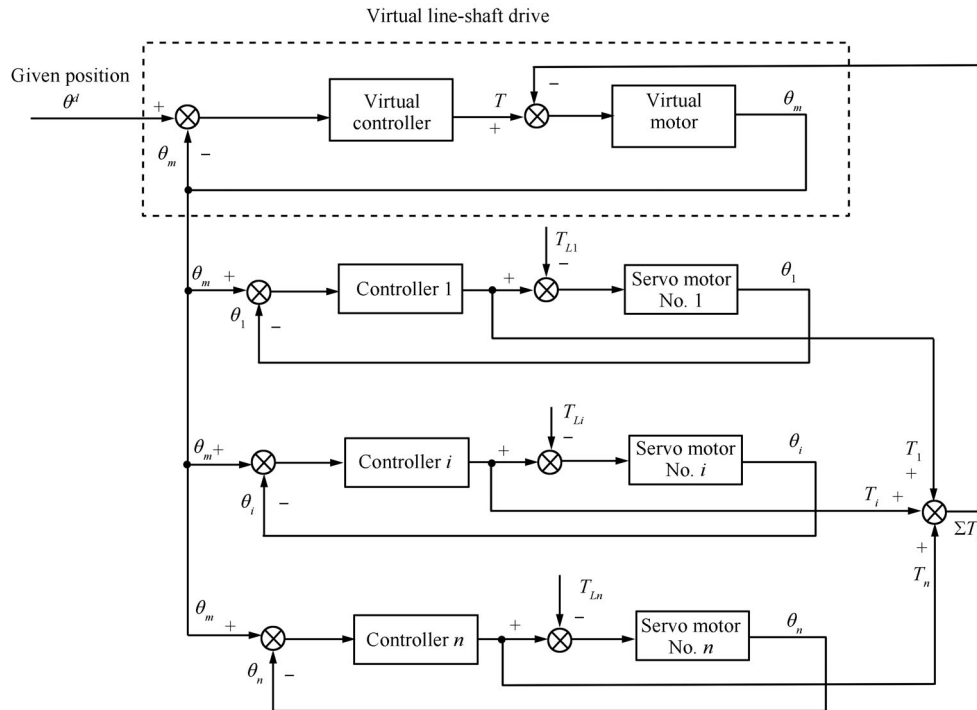

Fig. 1　Structure of traditional ELS system

to its slaves. Under steady-state conditions, every axis follows the virtual shaft, and excellent synchronization performance can be achieved. If one or more axes deviate from the reference value due to a disturbance, torque integration and feedback enables the virtual shaft to sense this variation and produce an adjusted reference value for the other slaves. In this manner, synchronization is always achieved among the axes. The torque balancing equation is

$$T - \sum T_i = J_m \ddot{\theta}_m \tag{7}$$

where T, J_m, θ_m are the driving torque, the inertia and the angular position of the virtual shaft, respectively, T_i $(i=1,2,\cdots,n)$ is the feedback restoring torque from each physical axis, namely, virtual load torque. Payette defined virtual load torque as[8]

$$T_i = b_r \Delta\omega + k_r \Delta\theta + k_{ir} \int \Delta\theta \, \mathrm{d}t \tag{8}$$

where b_r is the damping gain, k_r is the stiffness gain, k_{ir} is the integrated stiffness, $\Delta\omega$ is the angular velocity error, and $\Delta\theta$ is the angular position error.

4 Synchronization control strategy of ELS with observer

Because the load torque of the servo drive T_{li} $(i=1,2,\cdots,n)$ is time-varying and unpredictable, the traditional ELS control strategy integrates the virtual load torque of each axis T_i $(i=1,2,\cdots,n)$ as the torque feedback on virtual shaft, with which the motion synchronization is

harmonized among axes. This virtual load torque is obtained by calculating the virtual stiffness gain and damping gain with the error between the system reference value and the actual output value (velocity or position error). Under steady-state conditions, the system error can be eliminated by properly designing the tracking controller of each axis. However, if a severe load disturbance occurs in the system, asynchronization probably happens among the axes due to the time delay caused by calculation of the virtual load torque. To solve this problem, a load observer is designed in this research, and the observed value is taken as the torque fed back to virtual shaft for the motion synchronization among the axes. This way reflects the dynamic relationship among the axes in a more precise manner. In this case, the torque balancing equation is

$$T - \sum \hat{T}_{Li}^* = J_m \ddot{\theta}_m \tag{9}$$

where $\hat{T}_{Li}^*$ $(i=1, 2, \cdots, n)$ is the estimation value of the equivalent load torque. A block diagram of the improved ELS control topology is shown in Fig. 2.

5 Observer design for synchronization system

Fig. 2 shows that every servo drive unit under the control of virtual shaft has symmetric structure. Therefore, the same control algorithm can be applied to each of them. Taking axis 1 for example, the design of a tracking controller and an equivalent load-torque observer for servo motor No. 1 is described in this section.
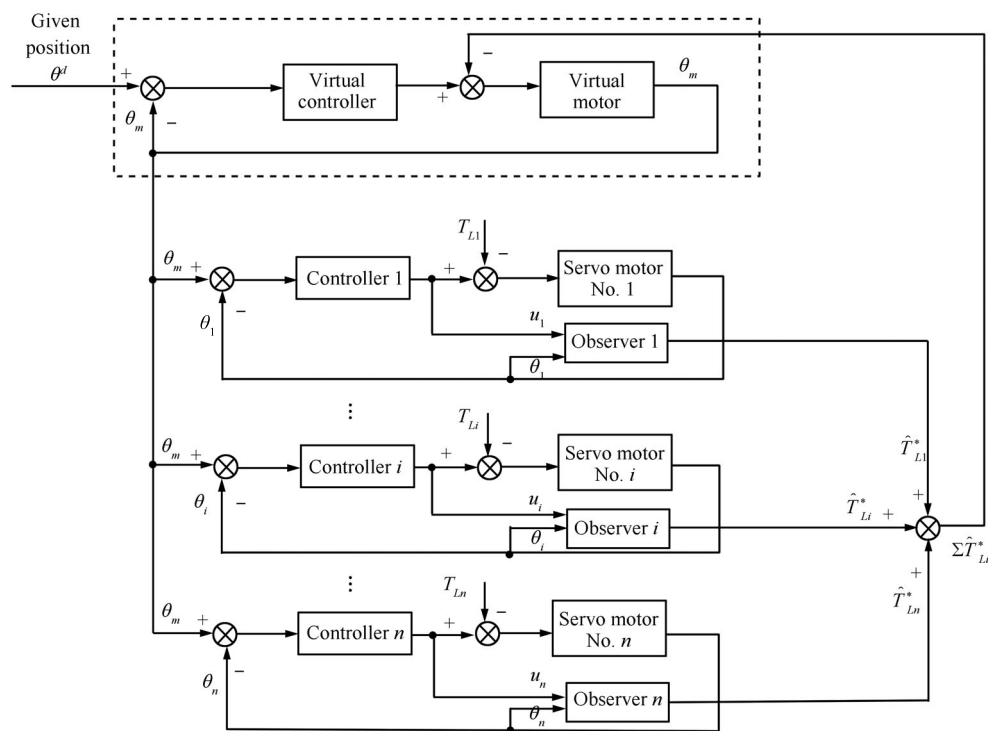

Fig. 2   Structure of improved ELS system

5.1 Design of the tracking controller

For a shaftless driven printing machine, each paper roller is driven by an independent servo motor, and in case of chromatic aberration, register control is carried out. These lead to higher requirements on multi-axis synchronization control in which the driving motor is considered as a complex object with nonlinear and variable parameters. With common PID control, satisfactory speed regulation and positioning are hard to achieve due to the weak robustness to disturbances and parameter variations.

In contrast, with the sliding-mode variable structure control, a type of nonlinear and discontinuous control, the system is capable to obtain excellent robustness which is actually called invariability through keeping motion within sliding surface[16]. Together with its simplicity, high real-time performance, and easy implementation, this method applied to high-precision tracking control has attracted significant attention[17]. This section describes the design of a sliding-mode controller for a single-axis system which guarantees not only the excellent tracking performance but also the high performance of observer. Moreover, it is also applicable to a multi-axis system with symmetrical motors.

As shown in Fig. 2, θ_m is the reference position of axis 1, and (1) shows that $x_1 = \theta_1$, thus the tracking error can be $e = \theta_m - x_1$.

Choose the linear sliding surface

$$s = ce + \dot{e} \tag{10}$$

where c indicates the slope of the sliding surface and is a positive constant need to be designed.

The output of the sliding mode controller can be obtained from (6) and (10) so that

$$u(t) = \frac{1}{\bar{b}} \left[c\dot{e} + \ddot{\theta}_m + \beta(x,t)\text{sgn}(s) + ks - \bar{a}_1 x_2 - \bar{a}_2 F_f(t) \right] \tag{11}$$

where k is a positive constant and $\beta(x,t)$ is the switched gain. Both of them need to be designed. $\text{sgn}(\cdot)$ is the signum.

Assume that T_L^* is unknown but bounded and subject to $|T_L^*| \leq M$, where the positive constant M is known.

If design

$$\beta(x,t) = M + \eta \tag{12}$$

then $s\dot{s} = -\eta |s| - ks^2 \leq 0$, which means that the reachability condition is satisfied, and a sliding mode motion on s is attainable in finite time, where η is also a positive constant.

A sigmoid function $\lambda(s)$ is used instead of the signum function $\text{sgn}(s)$ as the switching function in order to reduce the effect of chattering which occurs on the sliding surface[18]. The sigmoid function is defined as

$$\lambda(s) = \frac{2}{1 + \text{e}^{-as}} - 1 \tag{13}$$

where a is a positive constant used to regulate the slope of the sigmoid function.

5.2 Design of the observer

From (6), the sliding mode observer is designed as

$$\begin{cases} \dot{\hat{x}}_1 = \hat{x}_2 + v_1 \\ v_1 = L_1\text{sgn}(x_1 - \hat{x}_1) \end{cases} \tag{14}$$

$$\begin{cases} \dot{\hat{x}}_2 = \bar{a}_1\hat{x}_2 + \bar{b}u(t) + \bar{a}_2 F_f(t) + v_2 \\ v_2 = L_2\text{sgn}(x_2 - \hat{x}_2) \end{cases} \tag{15}$$

where L_1 and L_2 are two positive constants to be designed later.

Define the estimation errors of the observer as

$$\begin{cases} e_1 = x_1 - \hat{x}_1 \\ e_2 = x_2 - \hat{x}_2. \end{cases} \tag{16}$$

From (6), (14)−(16), the error equation can be obtained as

$$\begin{cases} \dot{e}_1 = e_2 - v_1 \\ \dot{e}_2 = \bar{a}_1 e_2 + T_L^* - v_2. \end{cases} \tag{17}$$

Proposition 1. Consider the system described by (6) and its observers described by (14) and (15). If L_1 and L_2 are sufficiently large, then the estimated equivalent load torque can be obtained by $\hat{T}_L^* = L_2\text{sgn}\left[L_1\text{sgn}e_1\right]$.

Proof.

The first step: Define the sliding surface

$$s_1 = e_1 \tag{18}$$

The second step: Choose the Lyapunov function $V_1 = \frac{1}{2}e_1^2$.

Along the trajectory of system (17), the derivative of the Lyapunov function with respect to time is

$$\begin{aligned} \dot{V}_1 = e_1\dot{e}_1 &= e_1 e_2 - e_1 v_1 = \\ & e_1 e_2 - e_1 L_1\text{sgn}e_1 = \\ & e_1 e_2 - L_1 |e_1| \leq \\ & |e_1||e_2| - L_1 |e_1| = \\ & |e_1|\left[|e_2| - L_1\right]. \end{aligned} \tag{19}$$

When $L_1 \geq |e_2|$ by design, there is $\dot{V}_1 \leq 0$, i.e., $s_1\dot{s}_1 \leq 0$. It means that the reachability condition is satisfied, and a sliding-mode motion on s_1 is attained in finite time. According to the equivalence principle of the sliding-mode theory, it follows that

$$s_1 = \dot{s}_1 = 0. \tag{20}$$

Then, from (14)−(18), (20),

$$e_2 = L_1\text{sgn}e_1. \tag{21}$$

Now e_2 can be expressed using (21).

The third step: Define the sliding surface

$$s_2 = e_2. \tag{22}$$

The fourth step: Choose the Lyapunov function $V_2 = \frac{1}{2}(e_1^2 + e_2^2)$, then

$$\dot{V}_2 = e_1\dot{e}_1 + e_2\dot{e}_2 = \dot{V}_1 + e_2\dot{e}_2. \tag{23}$$

Applying the same reasoning as in the proof of the second step, we obtain $\dot{V}_2 \leq e_2\dot{e}_2$.

Then, from (17)

$$\dot{V}_2 \leq e_2\dot{e}_2 = \bar{a}_1 e_2^2 + |e_2|\left[T_L^* - L_2\right] = \\ -|\bar{a}_1|\,e_2^2 + |e_2|\left[T_L^* - L_2\right]. \tag{24}$$

When $L_2 \geq |T_L^*| \geq M$ by design, there is $s_2\dot{s}_2 \leq 0$. It means that the reachability condition is satisfied and a sliding-mode motion on s_2 is attained in finite time. According to the equivalent principle of the sliding-mode theory, it follows that

$$s_2 = \dot{s}_2 = 0. \tag{25}$$

The estimated value of the equivalent load torque can be obtained from (14)–(18), (23) and (25):

$$\hat{T}_L^* = v_2 = L_2\mathrm{sgn}e_2 = L_2\mathrm{sgn}\left[L_1\mathrm{sgn}e_1\right]. \tag{26}$$

$\square$

Now the load torque T_L and the uncertain items caused by parameter variation can be obtained from (26).

Based on the above analysis, the procedure of observer design for system synchronization can be summarized as follows:

Step 1. Design the system control algorithm of a single-axis system according to (11) in order to maintain the tracking performance of the system.

Step 2. Replace the sgn(s) in (11) with the sigmoid function in (13) in order to minimize sliding-model chattering. This chattering reduction method will be used again in the subsequent design.

Step 3. Construct the observer according to (14) and (15) and calculate the estimated value of equivalent load torque according to (26).

Step 4. Carry out ELS synchronization control according to Fig. 2 and (9).

6 Experiments

6.1 Setting experimental parameters

Taking a four-axis printing machine with shaftless drive for example, a Matlab simulation model was built. Considering that in printing machine, the strong system non-linearity only happens during the low speed pre-register stage, a low-amplitude, low-frequency sinusoidal signal $\theta_d = 0.1\sin(2\pi t)$rad is used as the given position signal. By choosing the nominal values of the system as $F_c = 15\,\mathrm{N \cdot m}$, $k_v = 2.0\,\mathrm{N \cdot m \cdot s/rad}$, $F_m = 20\,\mathrm{N \cdot m}$, $\sigma_1 = 0.01$ and $\sigma_2 = 0.1$. DC motor parameters are shown in Table 1. And the corresponding control system parameters are $c = 30$, $k = 5$, $a = 50$, $M = 10$, $\eta = 10$, $L_1 = 20$ and $L_2 = 100$.

Table 1 DC motor parameters

Parameters	Motor 1	Motor 2	Motor 3	Motor 4
R	7.77	6.5	8.67	8.25
k_m	6	4	7	6
c_e	1.2	1.0	1.2	1.0
k_u	11	11	11	11
J	0.6	0.4	0.8	0.5
F_m	20	15	30	28
F_c	15	10	25	24
k_v	2.0	1.5	4.0	3.0
$[\theta,\ \omega]$	$[-0.5; 0]$	$[-0.2; 0]$	$[0.25; 0]$	$[-0.25; 0]$

6.2 Analysis of the experimental results

6.2.1 Case 1. Tracking performance

Use the sinusoidal signal $\sin(4t)$ to simulate the disturbance of system parameters R and J, and a 2 N step signal added on axis 1 at the moment of 1 s to simulate an abrupt load change. The position tracking results and the observed results of the equivalent load observer for a single-axis system are shown in Figs. 3 and 4, respectively. Fig. 3 shows that with the use of a sliding-mode controller, the actual system value tracks the given value rapidly accompanied by excellent system robustness, and after $t > 2\,\mathrm{s}$, good tracking performance is obtained. Fig. 4 shows that the designed observed load-torque values converge within a short time. These results indicate that the control method satisfies control system requirements and lays a good foundation for multi-axis synchronization control as well.
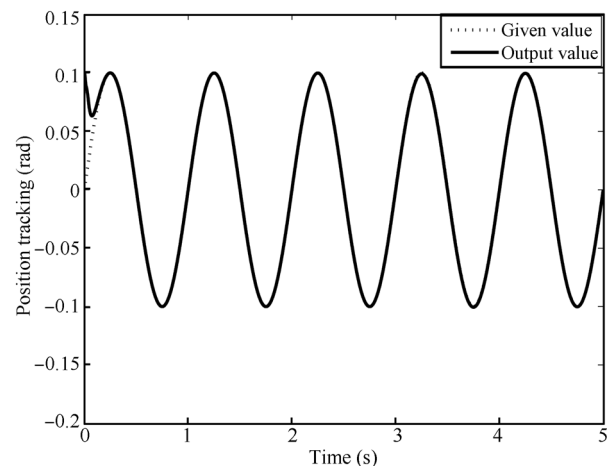

Fig. 3   Tracking performance of single-axis system

6.2.2 Case 2. Multi-axis synchronization coordination performance

To verify the effectiveness of the method proposed in this paper, a comparative experiment was performed based on the traditional ELS control method shown in Fig. 1 and the improved ELS control method shown in Fig. 2.
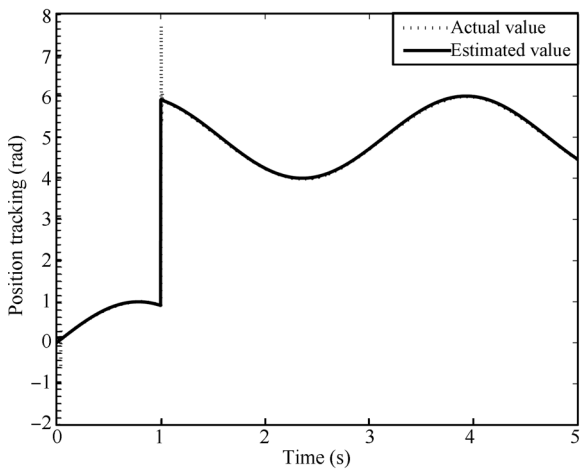
Fig. 4 Estimated value of the designed observer

1) Synchronization performance without disturbance.
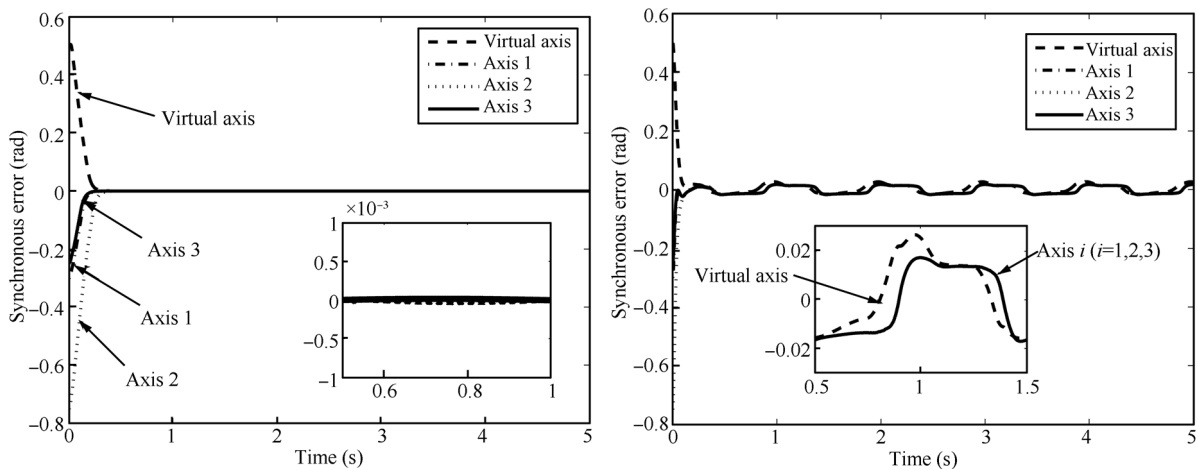
2) Synchronization performance with disturbance.

At 2 s, a 3 N step signal was added on axis 1 to simulate an abrupt load change.

As Fig. 5 shows, if there is no any external disturbance, both control schemes achieve excellent tracking performance by means of well-designed controllers. However, by examining the details shown in Figs. 6 and 7, it apparently shows that taking coupling torque as the torque feedback leads to a constant deviation between the main reference value and each axis, so that the tracking error of each axis deviates from zero to the balance point. It implies that the traditional ELS achieves high tracking performance with the cost of tracking performance loss in each axis.

In contrast, the improved ELS introduces a solution based on the equivalent load torque observer. By taking the observed value of the equivalent load torque as the torque feedback, the control system can guarantee not only high synchronization performance, but also excellent tracking performance on each axis. In addition, sliding-mode variable structure keeps system operation status stable in case of disturbance. Furthermore, it plays its role on improving overall robustness, steady-state performance, and synchronization performance.
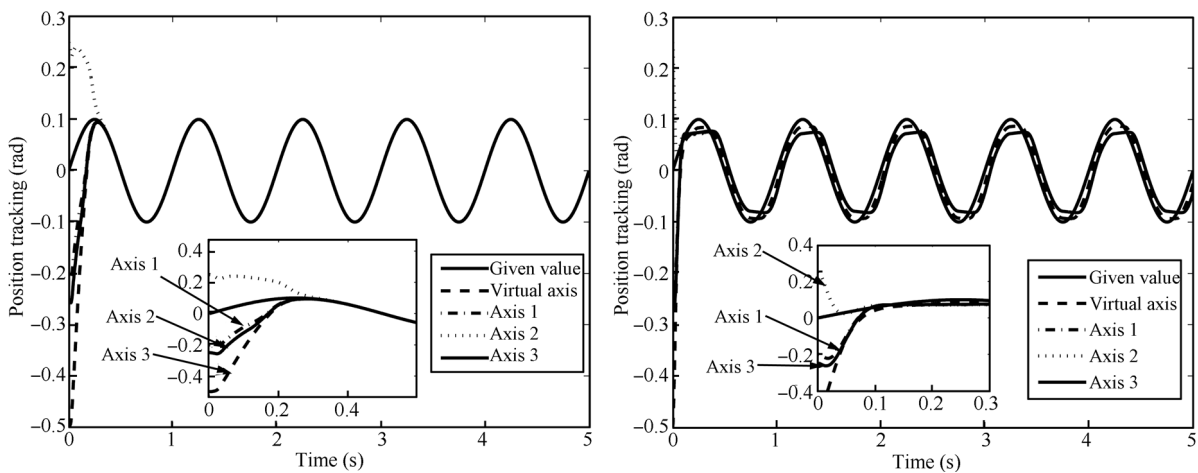
(a) Improved ELS control

(b) Traditional ELS control

Fig. 5 Tracking performance of multi-axis system without disturbance

(a) Improved ELS control

(b) Traditional ELS control

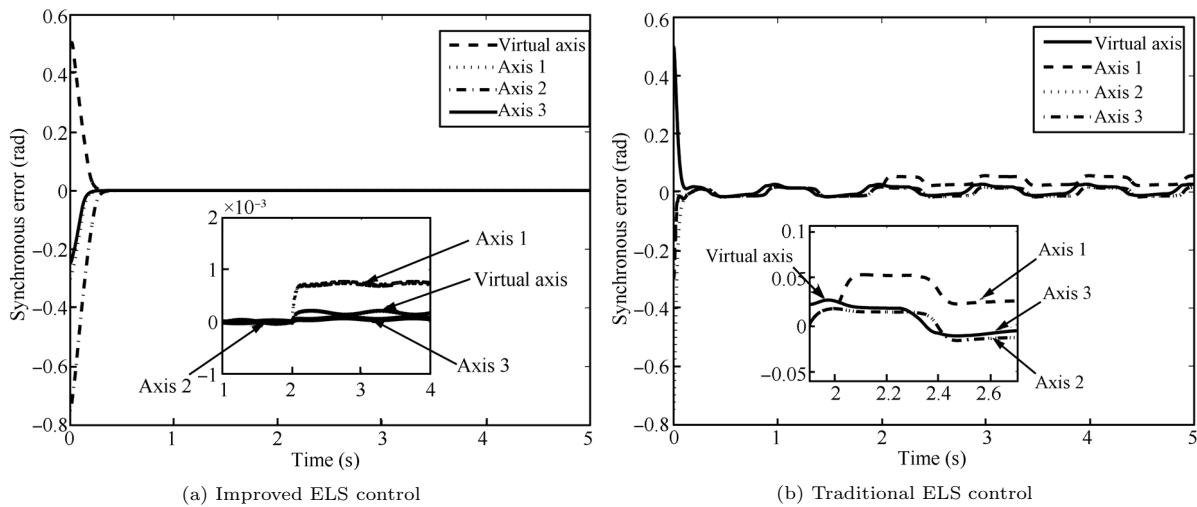Fig. 6 Synchronization errors of multi-axis system without disturbance

(a) Improved ELS control

(b) Traditional ELS control

Fig. 7   Synchronization errors of multi-axis system with disturbance

7   Conclusions

Focusing on improving the synchronization performance of traditional ELS control, an equivalent load observer based control strategy is proposed in this paper. First, sliding-mode controllers are designed for each axis in a multi-axis synchronization system to achieve high tracking performance and improve system resistance to disturbances. Second, the equivalent load-torque observer is designed to get the observer equivalent torque value of each axis for eliminating the constant deviation between the main reference value and each axis. This control strategy is especially helpful in maintaining synchronized motion control when severe load disturbances occur. Experimental results have demonstrated the effectiveness of the proposed control strategy for multi-axis systems when taking unexpected load disturbances into account during normal operations.

Acknowledgements

References

[1] Y. Xiao, K. Y. Zhu. Optimal synchronization control of high-precision motion system. *IEEE Transactions on Industrial Electronics*, vol. 53, no. 4, pp. 1160–1169, 2006.

[2] Z. H. Yu. Research on Synchronization Control Strategy of Shaftless System, Master dissertation, Northeastern University, China, 2008. (in Chinese)

[3] C. Chen, X. Q. Liu, G. H. Liu, L. Zhao, L. Chen, B. H. Zhao. Multi-motor synchronous system based on neural network control. In *Proceedings of the 11th International Conference on Electrical Machines and Systems*, IEEE, Wuhan, China, pp. 1231–1236, 2008.

[4] F. J. Pérez-Pinal, C. Nunez, R. Alvarez, I. Cervantes. Comparison of multi-motor synchronization techniques. In *Proceedings of the 30th Annual Conference of the IEEE Industrial Electronics Society*, IEEE, Busan, South Korea, pp. 1670–1675, 2004.

[5] M. A. Valenzuela, R. D. Lorenz. Startup and commissioning procedures for electronically line-shafted paper machine drives. *IEEE Transactions on Industry Applications*, vol. 38, no. 4, pp. 966–973, 2004.

[6] X. M. Li, P. X. Li. Research for synchronized control strategy based on virtual shaft control algorithm. *Chinese Hydraulics and Pneumatics*, no. 8, pp. 36–40, 2008. (in Chinese)

[7] R. D. Lorenz, P. B. Schmidt. Synchronized motion control for process automation. In *Proceedings of Conference Record of the 1989 Industry Applications Society Annual Meeting*, San Diego, USA, pp. 1693–1698, 1989.

[8] K. Payette. The virtual shaft control algorithm for synchronized motion control. In *Proceedings of the American Control Conference*, IEEE, Philadelphia, USA, pp. 3008–3012, 1998.

[9] K. Payette. Synchronized motion control with the virtual shaft control algorithm and acceleration feedback. In *Proceedings of the American Control Conference*, IEEE, San Diego, USA, pp. 2102–2106, 1999.

[10] A. Valenzuela, R. D. Lorenz. Electronic line-shafting control for paper machine drives. *IEEE Transactions on Industry Applications*, vol. 37, no. 1, pp. 158–164, 2001.

[11] F. J. Perez-Pinal. Improvement of the electronic line-shafting. In *Proceedings of the 35th Annual IEEE Power Electronics Specialists Conference*, IEEE, Aachen, Germany, pp. 3260–3265, 2004.

[12] C. M. Wolf, R. D. Lorenz. Digital implementation issues of electronic line shafting. *IEEE Transactions on Industry Applications*, vol. 46, no. 2, pp. 750–760, 2010.

[13] M. T. Huang, J. Ma. Research on tension control algorithm in shaftless-driven printing. In *Proceedings of the 3rd International Conference on System Science, Engineering Design and Manufacturing Information*, IEEE, Chengdu, China, pp. 109–112, 2012.

[14] S. S. Yeh, J. T. Sun. Design of perfectly matched zero-phase error tracking control for multi-axis motion control systems. In *Proceedings of the SICE Annual Conference*, IEEE, Akita, Japan, pp. 528–533, 2012.

[15] S. W. Lee, J. H. Kim. Robust adaptive stick-slip friction compensation. *IEEE Transactions on Industrial Electronics*, vol. 42, no. 5, pp. 474–479, 1995.

[16] A. Šabanovic. Variable structure systems with sliding modes in motion control— a survey. *IEEE Transactions on Industrial Informatics*, vol. 7, no. 2, pp. 212–223, 2011.

[17] A. Marouf, M. Djemai, C. Sentouh, P. Pudlo. A new control strategy of an electric-power-assisted steering system. *IEEE Transactions on Vehicular Technology*, vol. 61, no. 8, pp. 3574–3589, 2012.

[18] H. Kim, J. Son, J. Lee. A high-speed sliding-mode observer for the sensorless speed control of a PMSM. *IEEE Transactions on Industrial Electronics*, vol. 58, no. 9, pp. 4069–4077, 2011.
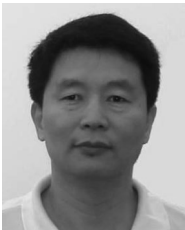
Chang-Fan Zhang received the M. Sc. degree from Southwest Jiaotong University China in 1989, and the Ph. D. degree from Hunan University, China in 2001. He is currently a professor at College of Electrical and Information Engineering, Hunan University of Technology, China.

His research interests include fault diagnosis on electric machines and industrial process control.
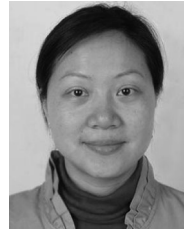
E-mail: zhangchangfan@263.net

ORCID iD: 0000-0002-9800-3984
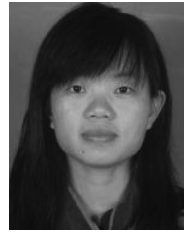
Yuan-Yuan Xiao graduated from Hunan University of Technology, China in 2011. She is currently a master student at the College of Electrical and Information Engineering, Hunan University of Technology, China.

Her research interest is fault diagnosis on electric machines

E-mail: xiaoyy3690@sina.com

Jing He received the M. Sc. degree from Central South University of Forestry and Technology, China in 2002, and the Ph. D. degree from National University of Defense Technology, China in 2009. She is currently a professor at the College of Electrical and Information Engineering, Hunan University of Technology, China.

Her research interests include fault diagnosis on mechatronics and industrial process control.

E-mail: hejing@263.net (Corresponding author)

ORCID iD: 0000-0002-3650-3270

Min Yan graduated from Hunan University of Technology, China in 2011. She is currently a master student at the College of Electrical and Information Engineering, Hunan University of Technology, China.

Her research interest is fault diagnosis on electric machines

E-mail: yanminhuixiao@163.com